Wrinkling of Pressurized Elastic Shells

Dominic Vella, Amin Ajdari, Ashkan Vaziri, and Arezki Boudaoud

Phys. Rev. Lett. **107**, 174301 — Published 20 October 2011

DOI: 10.1103/PhysRevLett.107.174301

Wrinkling pressurized elastic shells

Dominic Vella[1], Amin Ajdari[2], Ashkan Vaziri[2] and Arezki Boudaoud[3]
[1] *OCCAM, Mathematical Institute, University of Oxford, 24-29 St Giles', Oxford, OX1 3LB, UK*
[2] *Department of Mechanical and Industrial Engineering, Northeastern University, Boston, MA, 02115, USA*
[3] *Laboratoire Reproduction et Développement des Plantes & Laboratoire Joliot-Curie, INRA, CNRS, ENS, Université de Lyon, 46 Allée d'Italie, F-69364 Lyon Cedex 07, France*

We study the formation of localized structures formed by the point loading of an internally pressurized elastic shell. While unpressurized shells (such as a ping pong ball) buckle into polygonal structures, we show that pressurized shells are subject to a wrinkling instability. We study wrinkling in depth presenting scaling laws for the critical indentation at which wrinkling occurs and the number of wrinkles formed in terms of the internal pressurization and material properties of the shell. These results are validated by numerical simulations. We show that the evolution of the wrinkle length with increasing indentation can be understood for highly pressurized shells from membrane theory. These results suggest that the position and number of wrinkles may be used in combination to give simple methods for the estimation of the mechanical properties of highly pressurized shells.

PACS numbers: 46.32.+x, 46.70.De, 62.20.mq

The wrinkling of elastic membranes under tension is as important in a range of fields as it is visually arresting. In recent years, particular attention has been paid to the use of such wrinkling patterns to facilitate measurements in a wide range of settings from the traction forces exerted by fibroblasts during cell division [1] to the mechanical properties of the membranes themselves (such as Young's modulus and thickness) [2, 3]. There has also been considerable interest in understanding fundamental aspects of wrinkled membranes including the size and number of wrinkles [4–6], the transition from wrinkling to folding [7] and situations in which the wrinkle wavelength varies spatially [6, 8, 9].

For the most part, studies of wrinkling have considered planar sheets — objects without an intrinsic curvature. As every 'ping-pong' player knows, objects with an intrinsic curvature suffer a surprising mode of instability in which a large indentation localizes to form polygonal deformations [10] with ridges connecting vertices. These polygonal structures, occur in a wide range of applications from thin shells under point loading [11–14] through the drying of droplets of a colloidal suspension [15] to the oscillations of bubbles in echography [16]. Although polygonal structures and wrinkles may both be the manifestation of azimuthal instabilities of elastic objects subject to deformation, they are usually thought of as occurring in very different situations. In this Letter we show that it is possible to move continuously from polygonal structures to wrinkles within a single physical system: the indentation of an internally pressurized shell. We show that for 'small' internal pressures polygonal structures are observed giving way to wrinkles for 'large' internal pressures.

A simple demonstration of the azimuthal instability that develops when a pressurized shell is indented may be seen by pushing on a beach ball (see fig. 1); a large number of wrinkles form within an annulus of well-defined inner and outer radii. The indentation of pressurized elastic shells has recently received attention in its own right because of applications to drug delivery within polymeric capsules [17], the measurement of turgor pressure within yeast cells [18, 19] and the measurement of the mechanical properties of thin films [20].

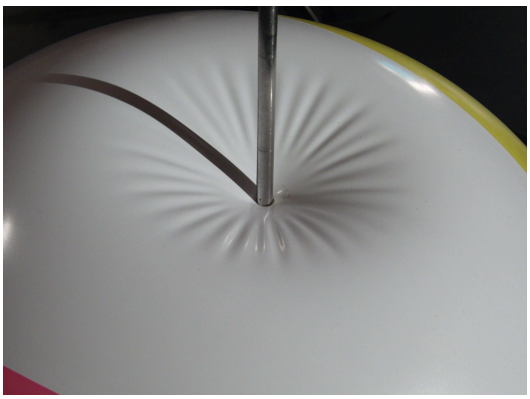

FIG. 1: The wrinkling of a beach ball under indentation.

To understand the wrinkling instability of pressurized shells demonstrated in fig. 1 we consider an elastic shell of natural radius R, thickness h, Young's modulus E, Poisson ratio ν and subject to an internal pressure (or pressure difference) p. The shell is then deformed by the action of a point-like force, F, at a pole. Numerical simulations were performed using the commercial finite element package ABAQUS (SIMULIA, Providence, RI) with material properties $R = 1$ m, $E = 70$ GPa and $\nu = 0.3$. (Three-node thin quadratic shell elements were used in all calculations and a mesh sensitivity study was carried out to ensure that the results are minimally sensitive to the element size.) These simulations reveal that for small vertical displacements, w_0, the response of the

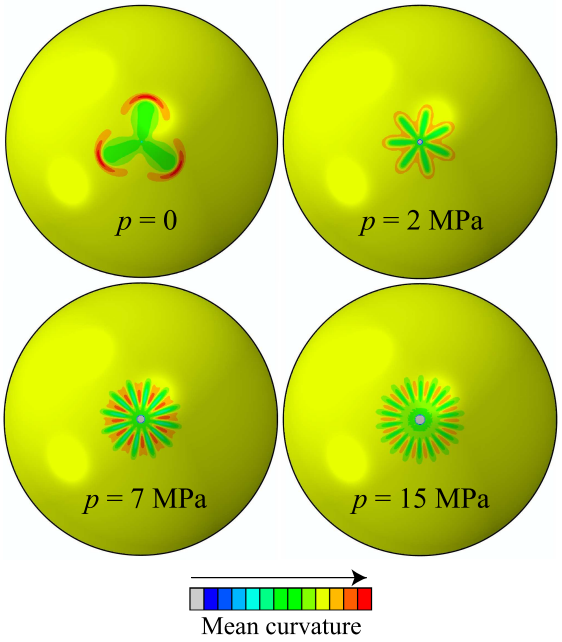

FIG. 2: (Color online) The transition from polygonal localizations to wrinkles with increasing internal pressure. Shading shows the mean curvature obtained in numerical simulations for a shell of radius $R = 1$ m, thickness $h = 2$ mm, Young's modulus $E = 70$ GPa and internal pressures $p = 0, 2, 7$ and 15 MPa. The corresponding values of the indentation are $w_0 = 0.1, 0.1, 0.22$ and 0.37 m, respectively.

shell remains axisymmetric but loses axisymmetry at a finite displacement, $w_0 = w_0^c$. Examples of the variation in the asymmetric pattern observed by varying just the internal pressure are shown in fig. 2. For unpressurized shells we observe polygonal structures, as studied previously. However, as the pressure increases the wavenumber of the asymmetry increases becoming reminiscent of the wrinkles observed when stretching a thin sheet [21, 22]. We note that these wrinkles are confined to an annular region and that as the indentation increases the size of this annulus increases but that the wavenumber, n, of the instability remains constant.

The numerical simulations motivate an investigation of the critical indentation required to initiate wrinkling, the number of wrinkles that form and the extent of the wrinkled region as indentation continues. As a first step, we use the equations of axisymmetric plate theory modified to incorporate the finite radius of curvature of the shell. These 'shallow-shell' equations are well known [23] and, in the polar geometry of interest here, take the form

$$B\nabla^4 w + \frac{1}{R}\frac{1}{r}\frac{\mathrm{d}}{\mathrm{d}r}\left(r\psi\right) - \frac{1}{r}\frac{\mathrm{d}}{\mathrm{d}r}\left(\psi\frac{\mathrm{d}w}{\mathrm{d}r}\right) = p \qquad (1)$$

and

$$\frac{1}{Eh}\frac{1}{r}\frac{\mathrm{d}}{\mathrm{d}r}\left\{r\frac{\mathrm{d}}{\mathrm{d}r}\left[\frac{1}{r}\frac{\mathrm{d}}{\mathrm{d}r}\left(r\psi\right)\right]\right\} = \frac{1}{R}\nabla^2 w - \frac{1}{2r}\frac{\mathrm{d}}{\mathrm{d}r}\left(\frac{\mathrm{d}w}{\mathrm{d}r}\right)^2 \qquad (2)$$

where $w(r)$ is the normal displacement of the shell (from the spherical state) and ψ is the derivative of the Airy stress function so that $\sigma_{\theta\theta} = \psi'$ and $\sigma_{rr} = \psi/r$. The bending stiffness of the shell is $B = Eh^3/12(1-\nu^2)$. Equations (1)-(2) are to be solved, in principle, with boundary conditions for the displacement $w(0) = -w_0$, $w'(0) = 0$, $w(r) \to 0$ as $r \to \infty$ and for ψ that $\psi'(r) - \nu\psi(r) \to 0$ as $r \to 0$ and $\psi \sim pRr/2$ as $r \to \infty$.

In the absence of pressure, $p = 0$, it is possible to non-dimensionalize the shell equations (1)-(2) using the shell thickness h and $(hR)^{1/2}$ as vertical and radial scales, respectively [24]. However, with $p > 0$ this non-dimensionalization breaks down. For maximum contrast with the unpressurized regime, our analysis will focus on the limit of large pressures p, for which a more natural radial scale is

$$\ell_p = \left(\frac{pR}{Eh}\right)^{1/2} R \qquad (3)$$

while vertical deflections are measured relative to ℓ_p^2/R [19, 24]. This non-dimensionalization introduces a dimensionless bending stiffness, τ^{-2} where

$$\tau = \frac{pR^2}{(EhB)^{1/2}} \sim \frac{p}{E}\left(\frac{R}{h}\right)^2 \qquad (4)$$

is a dimensionless measure of the tension within the shell due to inflation. In this formulation of the problem τ is the only dimensionless parameter and so it is natural to investigate the dimensionless indentation required to produce wrinkling and the number of wrinkles as functions of τ. Such a plot is shown in figure 3 for numerical simulations performed with a range of shell thicknesses and internal pressures. The very good collapse observed demonstrates that the parameter τ is indeed the universal governing parameter for this system. We now focus on understanding the observed behaviour in the limits $\tau \ll 1$ and $\tau \gg 1$.

We consider first the limit $\tau \ll 1$, which corresponds to very weakly pressurized shells and has been considered extensively previously. In this limit, the standard non-dimensionalization shows that localized structures must appear when the indentation $w_0 \sim h$. Numerical simulations (see fig. 4c of [14]) suggest that in fact $w_0^c \approx 14h$. Rewriting this result in dimensionless form we find that

$$\frac{w_0^c R}{\ell_p^2} \approx 14\frac{hR}{\ell_p^2} = 28\left[3(1-\nu^2)\right]^{1/2}\tau^{-1}. \qquad (5)$$

(More details may be found online [24].) This result is shown as the dotted line in fig. 3a demonstrating that (5), derived under the assumption that $\tau \ll 1$, is in fact valid for $\tau \lesssim 1$. In this limit we also expect that the wavenumber of the instability should be $n = 3$, as has been reported many times previously for unpressurized shells [10, 11, 13]. This is indeed the case for $\tau \ll 1$ (fig. 3b).

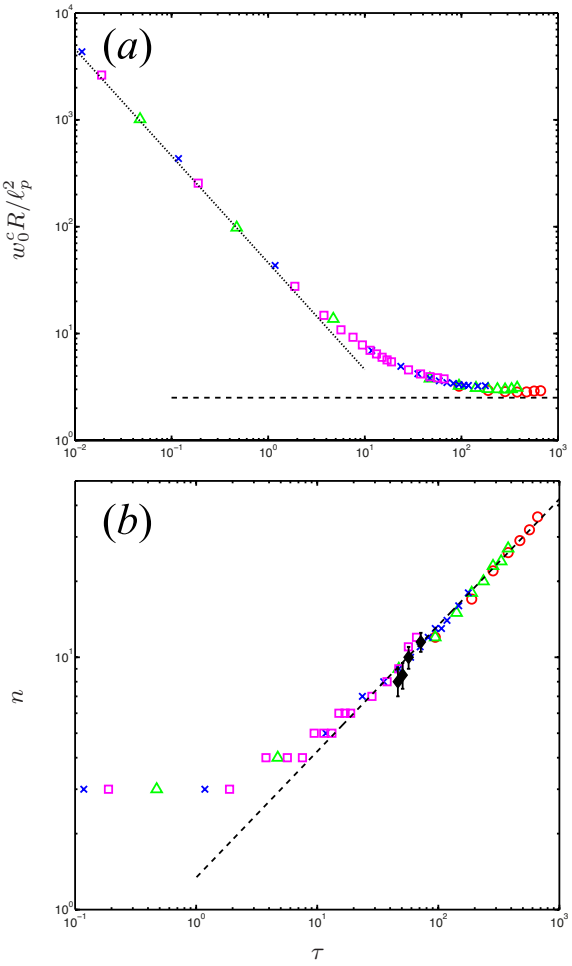

FIG. 3: (Color online) The onset of instability. Results from numerical simulations (points) are shown for shells with radius $R = 1$ m and thicknesses $h = 0.5$ mm (◯) 1 mm, (△), 2 mm (×) and 5 mm (□) with a range of internal pressures. (a) The critical displacement at which asymmetric deformation patterns are first observed. The dotted line shows the result (5), valid for $\tau \ll 1$. The dashed line shows the prediction of membrane theory that $w_0^c \approx 2.52\ell_p^2/R$. (b) The wavenumber of the asymmetric deformation pattern n. The dashed line shows the result (6) valid for $\tau \gg 1$, with a prefactor 1.33. Experimental measurements of the critical wavenumber for a Pezzi ball ($R = 18.5$ cm, $h = 1$ mm and $E = 2.3$MPa) inflated to different pressures are also shown (⧫).

In the limit $\tau \gg 1$, the bilaplacian term in (1) may be neglected leading to the dimensionless membrane-shell equations [19, 24]. In this membrane limit we expect that an azimuthal instability will be observed when the hoop stress becomes compressive, i.e. $\psi' = \sigma_{\theta\theta} < 0$. The numerical solution of the membrane-shell equations for increasing values of $w_0 R/\ell_p^2$ suggests that $\sigma_{\theta\theta} = 0$ first occurs when $w_0 R/\ell_p^2 \approx 2.52$. Furthermore, this root occurs with $r/\ell_p = r_c/\ell_p \approx 0.58$. The prediction from membrane theory that $w_0^c R/\ell_p^2 = 2.52$ is plotted as the dashed line in fig. 3a and is in good agreement with the numerical simulations as $\tau \to \infty$. We also note from fig. 3a that, in dimensional terms, increasing the internal pressure delays the onset of instability.

In the strongly pressurized regime, we expect that the wavenumber of wrinkles should be described by a balance between bending and stretching [21, 22]. In our case, this balance (see the governing equations (1)-(2)) yields a typical wavelength of wrinkles $\lambda \sim (BR^2/Eh)^{1/4} \sim (hR)^{1/2}$. Since we are considering the limit $\tau \gg 1$ we expect that the typical radial extent of the wrinkled region will be $\sim \ell_p$ so that the wavenumber of the wrinkles, $n \sim \ell_p/\lambda$ is given by

$$n \sim \tau^{1/2}. \tag{6}$$

This relationship is observed in numerical simulations (see fig. 3b) with a prefactor ≈ 1.33, though the value of n is limited to taking integer values. Figure 3b also shows the results of experiments using an inflated Pezzi ball (Ledragomma), which agree well with the results of simulations for a very different series of physical parameters. We note that the transition from a small number of vertices to a large number of wrinkles as τ increases is smooth and does not occur at a well-defined value of τ. (The smooth nature of this transition is also seen in the behaviour of the excess mean curvature along the length of one asymmetric structure [24].)

A quantity of considerable interest is the size of the wrinkled region as the displacement is increased beyond the onset of wrinkling. The pure membrane model ($\tau = \infty$) suggests that the hoop stress is compressive within an annulus $L_{in} < r < L_{out}$ and hence that wrinkling will occur within the same annulus. Such an annular region is observed in both experiments (fig. 1) and simulations (fig. 2). The dependence of L_{in} and L_{out} on the dimensionless indentation may be computed from the membrane equations [24]; the results of this analysis are shown in fig. 4 along with the results of simulations for finite values of τ. This demonstrates that the simple membrane analysis gives an adequate description of the wrinkling in this situation, unlike some related wrinkling problems [3, 25], in which the presence of wrinkles significantly modifies the stress field [26].

A boundary layer analysis of the membrane-shell equations [19, 24] shows that for very large displacements the Airy stress function is given asymptotically by $\psi \approx p|w_0 R - r^2|/2r$. Since the behaviour near $r = (w_0 R)^{1/2}$ is smoothed by a geometrical boundary layer, $\sigma_{\theta\theta} = 0$ at $r = (w_0 R)^{1/2}$ and hence, for $w_0 R/\ell_p^2 \gg 1$, the outer position of the wrinkles is given approximately by

$$L_{out} \approx (w_0 R)^{1/2}. \tag{7}$$

This result is recovered in the numerical results (see fig. 4) and is noteworthy because it is solely dependent on the geometry of the problem and is independent of the internal pressurization. Mathematically, (7) is identical to the corresponding result for unpressurized shells [13].

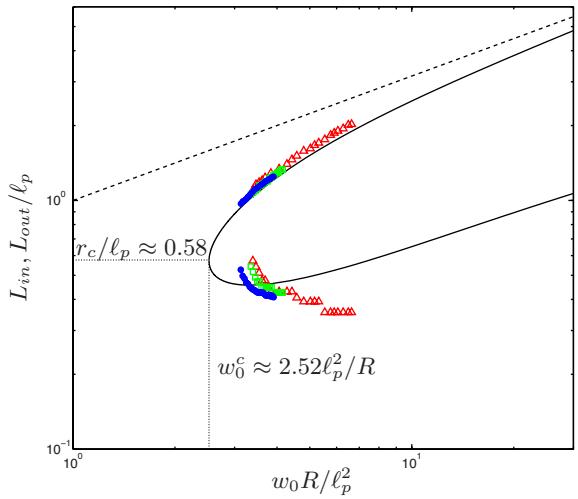

FIG. 4: (Color online) Evolution of wrinkle length with continuing indentation. The results from numerical simulations (points) are shown for shells with radius $R = 1$ m and thicknesses $h = 1$ mm (filled symbols) and $h = 2$ mm (open symbols). The internal pressure $p = 8$ MPa (●) $p = 9$ MPa (□) and 15 MPa (△). The prediction from the numerical solution of the membrane-shell model ($\tau = \infty$) is shown (solid curve) along with the asymptotic result (7) (dashed line), which is obtained as the $w_0 R/\ell_p^2 \gg 1$ limit of the membrane-shell theory. The onset of the asymmetric instability is illustrated by the dotted vertical and horizontal lines.

Wrinkling has previously been used as a simple means of measuring the material properties of nanometric planar membranes [3]. However, this study was hampered by the lack of a theoretical understanding of the wrinkling pattern that resulted and, despite more recent attempts [25], the wrinkling of these membranes is not completely understood. Motivated by the same desire, we note that the number of wrinkles observed gives a simple method of estimating the value of τ, under the assumption that $\tau \gg 1$ (which is the case if $n \gg 1$). If the material properties of the shell (E, h and R) are known then the interior pressure p may be determined using (6). This is significantly simpler than current techniques, which rely on measuring the force-displacement relationship [18, 19]. If only some of the material properties are known then other features of the wrinkling pattern, e.g. the radial position of wrinkles r_c, provide additional information that may be used for this inference.

We have considered the indentation of a pressurized elastic shell and shown that at low pressures ($\tau \ll 1$) the deformation localizes with the formation of polygonal structures while at higher pressure ($\tau \gg 1$) asymmetrical localization occurs with the formation of wrinkles. To our knowledge, this system is the first that is able to demonstrate both of these forms of localization with a single control parameter, in this case the dimensionless tension τ. We have also shown that the presence of an internal pressure increases the critical indentation w_0^c required to observe localization. Finally, an analysis of this system based on the equations of membrane-shell theory allowed us to obtain a more complete understanding of the wrinkle length than has been achieved in related systems [3, 25]; this wrinkling instability may be a useful assay for the determination of the mechanical properties of polymeric capsules.

This publication was based on work supported in part by Award No. KUK-C1-013-04, made by King Abdullah University of Science and Technology (KAUST). A.A. and A.V. are thankful for the support of NSF CMMI grant award #1065759. A.B. was supported by ANR-10-BLAN-1516. We are grateful to E. du Pontavice for his assistance with the experimental aspects, M. Hallworth for help with fig. 1 and B. Davidovitch for discussions.

[1] K. Burton and D. L. Taylor, Nature **385**, 450 (1997).
[2] C. M. Stafford *et al.*, Nature Mater. **3**, 545 (2004).
[3] J. Huang *et al.*, Science **317**, 650 (2007).
[4] J.-C. Géminard, R. Bernal, and F. Melo, Eur. Phys. J. E **15**, 117 (2004).
[5] E. Cerda, J. Biomech. **38**, 1598 (2005).
[6] H. Vandeparre *et al.*, Phys. Rev. Lett. **106**, 224301 (2011).
[7] D. P. Holmes and A. J. Crosby, Phys. Rev. Lett. **105**, 038303 (2010).
[8] J. Huang *et al.*, Phys. Rev. Lett. **105**, 038302 (2010).
[9] R. D. Schroll *et al.*, Phys. Rev. Lett. **106**, 074301 (2011).
[10] L. Pauchard and S. Rica, Phil. Mag. B **78**, 225 (1998).
[11] J. R. Fitch, Int. J. Solids Structures **4**, 421 (1968).
[12] A. V. Pogorelov, *Bending of Surfaces and Stability of Shells* (AMS Bookstore, Providence, RI, 1988).
[13] A. Vaziri and L. Mahadevan, Proc. Natl. Acad. Sci. USA **105**, 7913 (2008).
[14] A. Vaziri, Thin Wall. Struct. **47**, 692 (2009).
[15] N. Tsapis *et al.*, Phys. Rev. Lett. **94**, 018302 (2005).
[16] P. Marmottant *et al.*, J. Acoust. Soc. Am. **129**, 1231 (2011).
[17] V. D. Gordon *et al.*, J. Am. Chem. Soc. **126**, 14117 (2004).
[18] J. Arfsten *et al.*, Colloids Surf. B: Biointerfaces **79**, 284 (2010).
[19] D. Vella *et al.*, J. R. Soc. Interface, 10.1098/rsif.2011.0352(2011).
[20] R. Bernal *et al.*, Eur. Phys. J. E **34**, 13 (2011).
[21] E. Cerda and L. Mahadevan, Phys. Rev. Lett. **90**, 074302 (2003).
[22] E. Cerda *et al.*, Nature **419**, 579 (2002).
[23] C. R. Calladine, *Theory of Shell Structures* (Cambridge University Press, Cambridge, UK, 1983).
[24] See EPAPS Document No. XXX. For more information on EPAPS, see http://www.aip.org/pubservs/epaps.html.
[25] D. Vella *et al.*, Soft Matter **6**, 5778 (2010).
[26] M. Stein and J. M. Hedgepeth, *Analysis of Partly Wrinkled Membranes*, Tech. Rep. (NASA, 1961).